Impact of Rotational Speed and Impeller Types on Flow Patterns and Mixing Time in a Side-Entry Dual Mixer: A Study Using CFD and Visual Methods

Ardista Izdhihar Kaloka[a], Shendi Haris Firmansyah[a],
Marsyada Maghfirotul Wafiroh[a], Ni'mah Wati[a], Icha Nur Prayadi[a], Danawati Hari Prajitno[a*]

[a]*Department of Industrial Chemical Engineering, Faculty of Vocation, Sepuluh Nopember Institute of Technology, Surabaya 60111, Indonesia*
Corresponding author: dana@chem-eng.its.ac.id

Abstract
The effectiveness of industrial mixing processes is strongly influenced by impeller type and rotational speed because these parameters determine flow pattern, turbulence intensity, and fluid homogeneity. This study analyzes the effect of impeller type and rotational speed on flow pattern, mixing time, and turbulence characteristics in a side-entry dual mixer using a calcium carbonate ($CaCO_3$) suspension and water. The analysis was conducted using computational fluid dynamics (CFD) modeling and visual observation to identify circulation patterns and stagnant zones. Three impeller configurations were evaluated: dual four-blade propellers, four-blade pitched blade turbines (4-PBT), and a combination of both, operated at 300 and 600 rpm. The results show that impeller type significantly influences the flow pattern, while increasing rotational speed reduces mixing time. The dual 4-PBT at 600 rpm provided the best performance, characterized by multiple axial–radial circulation loops without stagnant zones and the fastest mixing time of 120 s. This configuration also produced the highest Reynolds number of 3127.19, indicating a transitional flow regime that enhances turbulence and accelerates homogenization. These results demonstrate the importance of selecting appropriate impeller types and rotational speeds to improve industrial mixing efficiency.

Keywords: Homogeneity; Impeller Type; Mixing; Rotational Speed

1. Introduction

Mixing is one of the most critical unit operations in various industrial processes, as it directly affects product quality, process efficiency, heat and mass transfer, and reaction performance [1]. In various industrial fields, mechanical mixing processes in stirred tanks play an important role, especially for solid- liquid mixing because they are capable of creating forced flow inside the vessel [2]. Mixing is the homogenization of two or more materials using an agitator to achieve uniformity [3]. The goal is to accelerate fluid homogeneity through mass and energy transfer, reduce differences in conditions, temperature, or other properties of a material, and prevent sedimentation [4]. The hydrodynamic characteristics in a mixing tank are influenced by the type, rotational speed, installation position, and geometry of the agitator and tank [5][6]. The agitator can be installed in the tank from the top, bottom, or side, depending on the tank's geometric design and fluid characteristics [7]. However, as tank capacity increases in industrial applications, achieving uniform mixing becomes more challenging due to increasingly complex flow distribution.

In large-capacity tanks, mixing challenges affect not only homogeneity but also operational energy requirements. Power consumption is influenced by the impeller configuration, rotational speed, fluid properties, and tank geometry; therefore, selecting the right impeller is crucial for improving mixing efficiency on an industrial scale [8]. Technically, the mixing principle refers to fluid mechanics and material transfer involving horizontal and vertical movement to improve the random distribution of components. The degree of mixing is assessed based on time, energy required, and uniformity level through sample testing [9]. Large-capacity stirred tanks do not allow the use of top entry mixing due to shaft installation limitations. This

Received : May 14, 2026
Accepted : July 14, 2026
DOI : 10.12962/j28075064.v12i1.a9682

is due to the use of a long shaft, which makes installation and maintenance more difficult on large-diameter tanks. Meanwhile, bottom entry agitator tanks are only suitable for use with high viscosity substances. In addition, its application is relatively limited to specific operating conditions [10]. Side Entry Mixers (SEM) are a type of side agitator tank that is designed to be more flexible for mixing liquids with various viscosities in large and small capacity tanks because the flow can cover the entire tank. SEM is also capable of producing more even circulation with a simpler installation than top-entry systems [11]. In addition, another advantage of this system is its low operational cost and the fact that no supports are required, making installation easy [5]. Compared to top-entry mixers, Side Entry Mixers (SEMs) are better suited for large-capacity tanks because they do not require a long vertical shaft, thereby reducing the risk of shaft deflection, the need for support structures, and installation complexity. In addition, SEMs generate strong horizontal circulation, enabling them to distribute the fluid throughout the tank, minimize stagnant zones, and maintain mixing homogeneity across large volumes [12]. Examples of side entry system applications are often found in the food industry, such as mixing milk with chocolate or flour with sugar [9].

Various studies have examined the impact of impeller rotation speed on mixing performance, one of which was conducted by Adnan *et al.* (2017), using a Computational Fluid Dynamics (CFD) approach. This study evaluated the velocity field in the tank to detect dead zones and found a positive correlation between rotational speed and increased flow fluctuations. This can occur because the higher the impeller rotational speed, the wider the fluid distribution, thereby narrowing the dead zone, vortex, and stagnant zone and maximizing the mixing process. However, this study has significant limitations because it is only relevant for low-density fluids due to the use of a top entry system with a single 3-blade mixer curve. In addition, the lack of experimental validation means that the accuracy of the simulation data cannot be fully confirmed. In addition, the study has not evaluated multi-impeller configurations in side-entry systems.

Meanwhile, Ahangari *et al.* (2016), studied the comparison between a 5-blade propeller impeller and a concave impeller in terms of mixing time in non-Newtonian fluids. The main finding of this research confirms that the most efficient variable for reducing mixing time is rotational speed; the higher the speed, the faster homogeneity is achieved. However, the scope of this study is still limited because it only analyzes the use of a single impeller configuration, so its application to dual or multiple impeller systems requires further study. The interaction between two types of impellers in a single mixing system has also not been studied.

More recent studies have focused on improving solid–liquid mixing performance through the optimization of impeller design and operating conditions. Xiong et al. (2022) investigated a dual axial impeller system by evaluating the effects of rotational speed, impeller configuration, and off-bottom clearance on solid suspension and mixing performance in a stirred vessel [13]. Ding et al. (2023) optimized a solid–liquid dual-impeller mixing system using CFD and PIV approaches to improve mixing efficiency and solid distribution [14]. However, these studies mainly focused on optimizing specific impeller configurations or dual impellers with similar designs, while the interaction between different impeller types remains insufficiently explored. In particular, investigations regarding combined impeller configurations in side-entry dual mixers for solid–liquid systems are still limited. Consequently, the influence of combined impeller configurations on hydrodynamic behavior, flow circulation, axial–radial flow interaction, turbulence generation, and overall mixing performance requires further investigation. This limitation highlights an important research gap that motivates the present study. Therefore, further research on impeller combinations in side-entry dual mixer systems is still needed.

To address this research gap, further investigation is needed to optimize the Side Entry Mixer (SEM) system, which offers broader application advantages than top-entry mixing systems, particularly for large-capacity stirred tanks. The novelty of this study lies in the evaluation of three dual-impeller configurations in a side-entry system using a visually validated CFD approach. The three impeller configurations were selected to represent different flow characteristics in the mixing system. Dual 4-blade propellers were expected to enhance axial circulation, dual 4-pitched blade turbines to increase axial-radial turbulence, and their combination to investigate the synergistic effect of both flow characteristics in improving flow patterns, reducing mixing time, and minimizing stagnant zones compared with a conventional single-impeller configuration [15], [16], [17]. Therefore, this study was designed to overcome the limitations of a single flow pattern by applying a dual mixer system modification to expand fluid distribution and minimize stagnant zones. Through a Computational Fluid Dynamics (CFD) approach validated experimentally using visual tracer particles (chia seeds), this study focuses on evaluating the influence of impeller types: dual 4-blade propeller, dual 4-pitched blade turbine, and their combination at rotational speeds of 300 and 600 rpm on flow pattern, mixing time, and turbulence level, thereby contributing to the optimization of large-scale industrial mixing system designs.

2. Materials and Methods

2.1. Materials

The materials used in this study included water at 25°C, 800 mesh $CaCO_3$, chia seeds, 0.1 N concentrated HCl, 0.1 N NaOH, Eriochrome Black T indicator, and 0.2 N EDTA.

2.2. Computational Fluid Dynamics (CFD) Procedures

Computational Fluid Dynamics is a computational method used to analyze fluid flow in machines, pipes, building structures, aerodynamics, and various other applications. The CFD process consists of three main stages: Pre- Processing, Processing, and Post-Processing [18].

2.2.1 Pre-Processing

The pre-processing stage began with the development of computational geometry based on the actual dimensions of the experimental stirred tank. The computational domain was divided into a stationary zone, representing the stationary tank, and a moving zone, representing the rotating impeller region. Subsequently, a computational mesh was generated for both zones to discretize the computational domain prior to the CFD simulation. The pre-processing stage is illustrated in Figure 1.

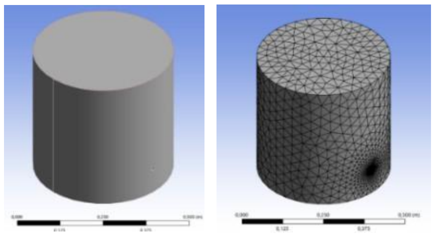

(a) (b)

Figure 1. Pre-Processing Stage (a) Geometric Modeling and (b) Grid Generation with Meshing

2.2.2 Processing

During the processing stage, the mesh generated in the pre-processing stage was imported into ANSYS Fluent, and the stationary and moving zones were combined using the append case procedure to establish the computational domain. A transient pressure-based solver was employed to capture the time-dependent flow characteristics during the mixing process. Turbulence was modeled using the Realizable k–ε model because of its capability to accurately predict turbulent recirculating and swirling flows commonly encountered in mechanically stirred tanks. The impeller rotation was represented using the Moving Reference Frame (MRF) approach, where the moving zone was defined using a rotational frame of reference, while the stationary zone was assigned an absolute frame of reference. Subsequently, the material properties, operating conditions, and boundary conditions were specified according to the experimental setup. The governing equations were solved using the Pressure-Implicit with Splitting of Operators (PISO) algorithm with appropriate solution control settings until convergence was achieved. Finally, solution animation was employed to visualize the transient evolution of the flow field and facilitate the analysis of flow patterns generated by different impeller configurations.

2.2.3 Post-Processing

The final stage was post-processing, in which the simulation results were obtained in the form of contour plots and numerical data for further analysis. The post-processing analysis included the evaluation of velocity contours, velocity vectors, streamlines, and flow circulation patterns to investigate the hydrodynamic characteristics generated by each impeller configuration. These CFD results were subsequently compared with the experimental flow visualization results to validate the numerical simulation and assess the agreement between the predicted and observed flow patterns.

2.3. Visual Procedures

Experimental flow visualization was conducted on a laboratory scale using the equipment setup shown in Figures 2 and 3. The equipment used consisted of an acrylic resin cylindrical tank placed inside a transparent box, intended to eliminate the effects of differences in refractive index between water and air [13]. Chia-seed tracer particles were introduced as passive tracers to visualize the fluid motion generated by different impeller configurations. The movement of the tracer particles was recorded using a DSLR camera and qualitatively analyzed to evaluate flow circulation, vortex formation, and stagnant zones, which were then compared with the CFD simulation results.

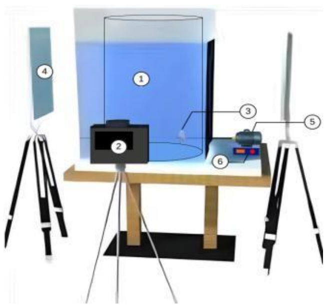

Figure 2. Visual Experiment Device Diagram

Description:
1. Side entry mixer tank with flat bottom measuring 40 x 60 cm
2. Digital Single Reflex Camera (DSLR)
3. Shaft and Impeller with 4-blade propeller and 4-pitched blade turbine with a diameter of 4 cm
4. Lighting using a light box
5. Motor
6. Impeller speed controller

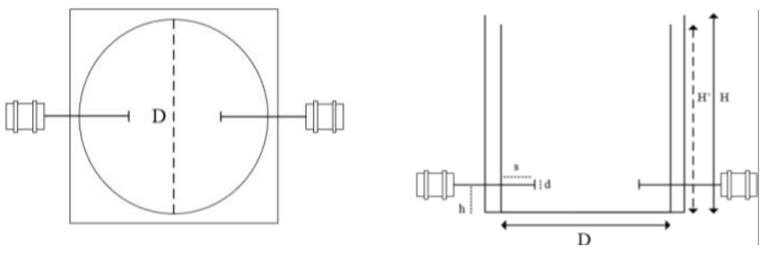

(a) (b)

Figure 3. Tank Geometry Dimension (a) Top View and (b) Front View

Table 1. Geometric Dimensions of the Side-Entry Mixer Tank

D	H	H'	h	d	s	d/D	h/d	s/D	β
40 cm	60 cm	40 cm	8 cm	4 cm	4 cm	0.1	2	0.1	0º

The main components of this setup were a 60 x 40 cm inlet-side cylindrical mixing tank with a variety of dual mixers: a 4-blade propeller, a 4-pitched blade turbine, and a combination of both types of impellers. The designs of the impellers used can be seen in Figure 4.

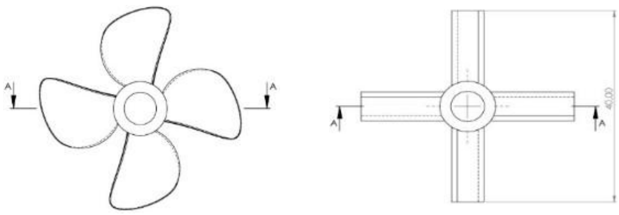

(a) (b)

Figure 4. Types of Impeller Used (a) 4-Blade Propeller and (b) 4-Pitched Blade Turbine

The experiment was conducted by filling the tank with room temperature water (25 °C) at atmospheric pressure. In addition, tracer particles were added to facilitate the analysis of the fluid flow pattern. The use of chia seeds as a tracer offers ease of visual observation, is non-hazardous, and does not interfere with the mixing process [19].

2.3.2 Identification of Flow Pattern Characteristics and Fluid Distribution Contours

Using visual techniques, objects moving linearly or circularly on a flat surface can be analyzed in terms of their velocity, acceleration, direction of motion, and position through Image Processing methods. The observations are captured as RGB color images using a DSLR camera. These images are then processed through Grayscale Processing using Adobe Photoshop. The resulting data are used to observe the tracer particle patterns with the aim of gaining a deeper understanding of the object's motion.

2.3.3 Measurement of Fluid Density

Sampling was conducted at the three predetermined points for measurement using a pycnometer. The suspension density was then calculated by subtracting the weight of the empty pycnometer (w1) from the weight of the pycnometer filled with the sample (w2), as determined using the following equation:

$$\rho s = \frac{w2 - w1}{Vp} \tag{1}$$

2.3.4 Determination of Fluid Concentration

In addition to density measurement, sampling was also carried out at the predetermined points to determine the sample concentration using the complexometric titration method. The principle of complexometry involves the formation of complex ions in solutions. In this stage, 10 ml of the sample was taken from each of the three points, followed by the addition of 2 drops of 0.1 N concentrated HCl, 2 ml of 0.1 N NaOH, and 3 drops of EBT indicator. The mixture was then titrated with 0.2 N EDTA solution until the color changed to blue. The sample concentration was subsequently determined using the following equation [20]:

$$\text{Concentration of CaCO3 (ppm)} = \frac{1000}{\text{V Sample}}\, x\ V\ EDTA\ X\ M\ EDTA\ X\ BM\ CaCO_3 \tag{2}$$

2.3.5 Determination of Homogeneity Value and Mixing Time

The homogeneity value represents the degree of uniformity between two or more fluids within a given area after the mixing process, with a maximum value of 1 indicating that the mixture concentration has become uniform. Homogeneity is determined from the sampling data with known density and involves the relationship between the homogeneity index and time. In this study, data were collected at 60-second intervals to ensure consistency and uniformity of the measurements.

2.3.6 Calculation of Reynolds Number

The Reynolds number (NRe) is a dimensionless quantity that refers to the ratio between inertial forces and fluid viscosity [21]. The Reynolds number is used to determine the turbulence level of a fluid, allowing the flow type to be predicted [22]. Based on flow characteristics, the Reynolds number is classified into three categories: laminar flow for NRe < 2100, turbulent flow for NRe > 4000, and transitional flow for NRe = 2100–4000 [23]. To classify the flow, the following equation is used [24]:

$$\mathrm{Re} = \frac{\rho D^2 N}{\mu} \tag{3}$$

Where N is the impeller rotational speed (rps), D is the impeller diameter (m), ρ is the fluid density (kg/m³), and μ is the viscosity (kg/m·s).

3. Results and Discussion

3.1. Result

Table 2. The Flow Patterns of Chia Seeds and Water by Impeller Types at Speeds of 300 and 600 rpm

Impeller Types	Methods	Rotational Speeds (rpm)	
		300	600
Dual 4-Blade Propeller	CFD	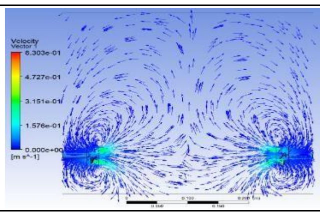	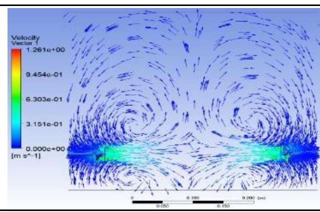
	Visual	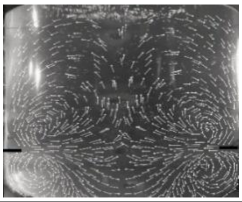	
Dual 4-Pitched Blade Turbine	CFD	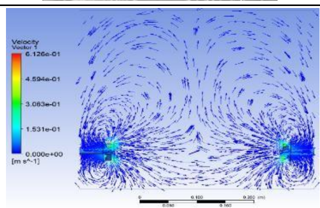	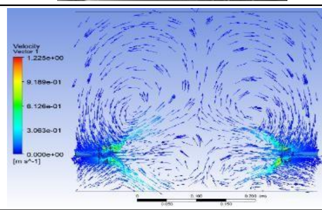
	Visual	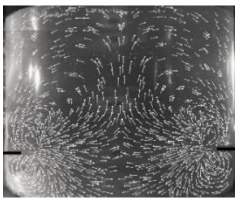	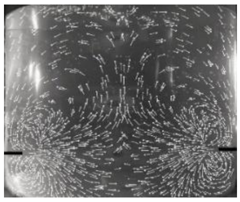

Both Combination	CFD	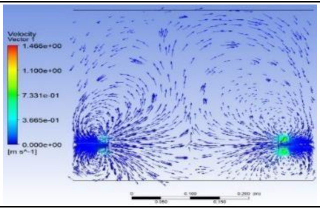	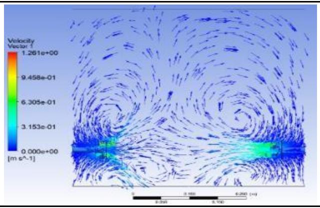
	Visual	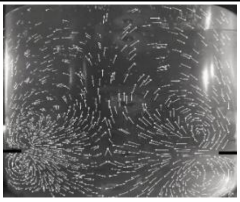	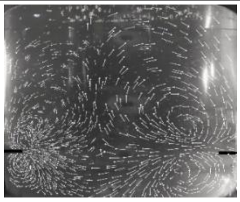

Table 3. The Distribution Contours of $CaCO_3$ and Water by Impeller Types at Speeds of 300 and 600 rpm

Impeller Types	Methods	Rotational Speeds (rpm)			
		300		600	
Dual 4-Blade Propeller	CFD	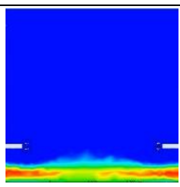 0 s	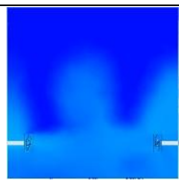 60 s	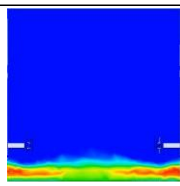 0 s	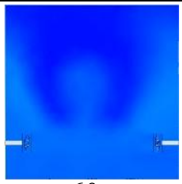 60 s
		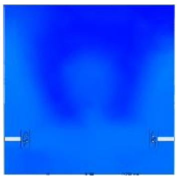 120 s	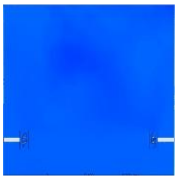 180 s	 120 s	 180 s
	Visual	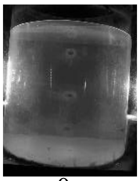 0 s	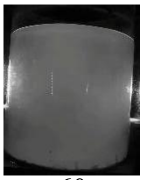 60 s	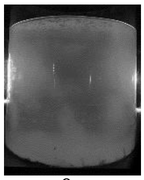 0 s	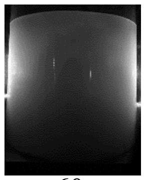 60 s
		 120 s	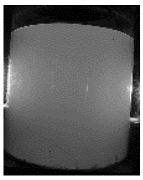 180 s	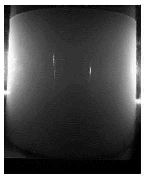 120 s	 180 s
Dual 4-Pitched Blade Turbine	CFD	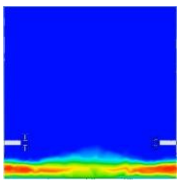	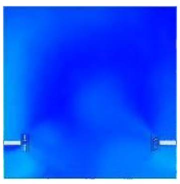	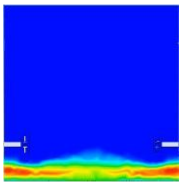	

0 s 60 s 0 s 60 s

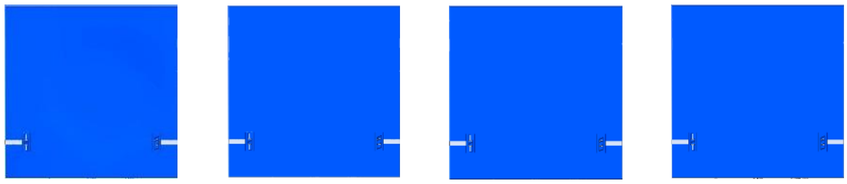

120 s 180 s 120 s 180 s

Visual

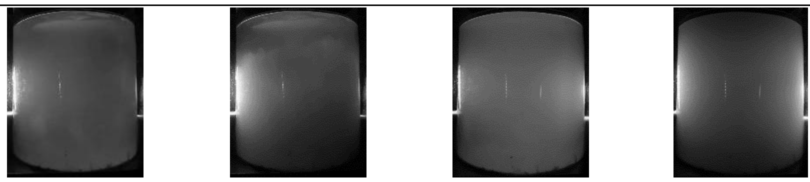

0 s 60 s 0 s 60 s

Impeller Types	Methods	Rotational Speeds (rpm) 300		Rotational Speeds (rpm) 600	

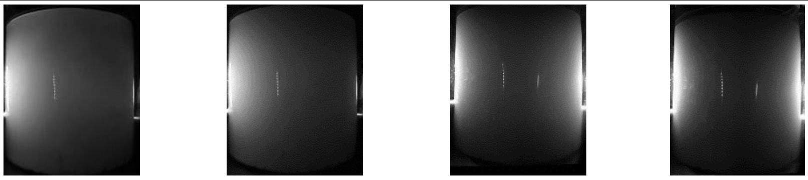

0 s 60 s 0 s 60 s

Both Combination

CFD

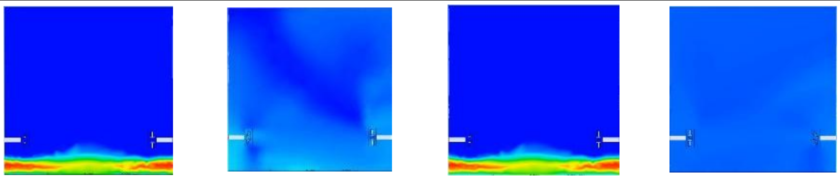

0 s 60 s 0 s 60 s

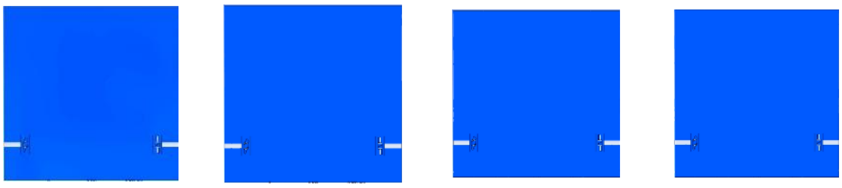

120 s 180 s 120 s 180 s

Visual

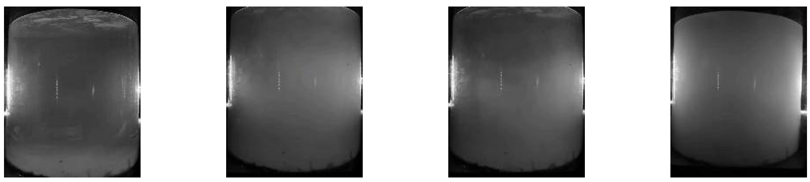

0 s 60 s 0 s 60 s

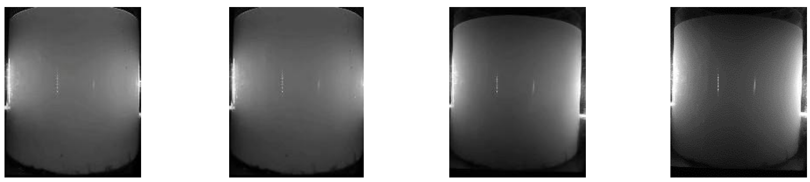

120 s 180 s 120 s 180 s

Table 4. Results of Homogeneity Value Calculation

Time (s)	Homogeneity Value					
	300 rpm			600 rpm		
	Dual 4-Blade Propeller	Dual 4-PBT	Both Combination	Dual 4-Blade Propeller	Dual 4-PBT	Both Combination
0	1.0000	1.0000	1.0000	1.0000	1.0000	1.0000
60	0.9980	0.9980	0.9989	0.9980	0.9974	0.9990
120	0.9994	0.9994	0.9990	0.9994	0.9994	0.9994
180	1.0000	1.0000	0.9994	1.0000	1.0000	1.0000

Table 5. Results of Reynolds Number Calculation

Impeller Types	Speed (rpm)	Speed (rps)	Density (Kg/m^3)	Viscosity (Kg/m.s)	NRe	In Re	Flow Type
Dual 4-Blade Propeller	300	5.00	1024.00	0.0052	1568.23	7.36	Laminar
	600	10.00	1024.70	0.0053	3068.86	8.03	Transitional
Dual 4-PBT	300	5.00	1024.50	0.0052	1584.65	7.37	Laminar
	600	10.00	1024.00	0.0052	3127.19	8.05	Transitional
Both Combination	300	5.00	1024.60	0.0053	1552.28	7.35	Laminar
	600	10.00	1025.73	0.0054	3042.55	8.02	Transitional

3.2 Discussion

Mixing is a process of homogenizing two or more substances using a mixer to achieve uniformity [3]. The selection of the type of agitator in the tank plays an important role in the mixing process, especially in accelerating fluid homogeneity. This study covers the effect of rotational speed and impeller type on flow patterns, mixing time, and turbulence level inside entry with dual mixers using Computational Fluid Dynamics (CFD) and visual methods. The results obtained from the three impeller types will be compared between Computational Fluid Dynamics (CFD) and visual methods for better design optimization to create an efficient mixing process.

3.2.1 The Effect of Rotational Speed and Impeller Type on Fluid Flow Patterns

The observation of flow patterns aims to identify vortices, fluid distribution circulation, and stagnant zones in the mixing process within the system, so that the level of mixing effectiveness can be determined. In the analysis of flow patterns, tracer particles are used to facilitate the identification of flow patterns. The results of flow pattern identification in the visual method will later be clarified with white arrows to facilitate reading the image. There are several factors that influence the formation of fluid flow patterns, namely: type, number of blades, and impeller rotation speed [4].

Based on Table 2, it can be seen that the fluid flow pattern using a 4-blade propeller forms a double loop circulation with a twin axial flow pattern, where the fluid flows parallel to the agitator [25]. This is indicated by the fluid from each impeller flowing out to the bottom of the tank towards the negative axis, then deviating and changing direction to move upwards towards the positive axis on the entire tank wall. The fluid then flows radially back into the negative axial direction towards the impeller, and the circular circulation ends [16]. The best flow pattern for the 4- blade propeller dual mixer variation was obtained at a speed of 600 rpm for each method. This is because the axial flow produced is strong enough to create an almost uniform fluid circulation throughout the tank volume, resulting in a very narrow stagnant zone at the upper right and left corners of the tank compared to a speed of 300 rpm. Stagnant zones are formed due to differences in viscosity between the fluid near the agitator, which tends to have lower viscosity, and the fluid far from the agitator, which has higher viscosity [26].

In the 4-PBT variation, multiple loop circulation is formed, namely there are 4 main circulations at the top and bottom of each mixer with a combination of axial-radial flow. This occurs due to the 45° angle of inclination on the turbine blades, as a result of which the top and bottom of the blades push the liquid in an axial direction, while the middle of the blades allows the liquid to be pushed in a radial direction. Turbine blades without tilt provide a radial flow effect that occurs due to the deflection of the flow horizontally towards the tank wall and then deflected upwards [27]. In this type, there is no stagnant zone, so the mixing process can occur more optimally because it covers the entire tank body. The best flow pattern in the dual mixer 4-pitched blade turbine variation was obtained at a speed of 600 rpm for each method, due to a faster and wider flow distribution compared to the 300 rpm speed variable.

Last, in the second combination of impeller types, it was found that all variables formed multiple loop circulation with axial flow (right) and axial-radial combination (left). On the right side, one circulation was formed with an axial flow pattern (4-blade propeller), and on the left side, two circulations were formed with a combined axial-radial flow pattern (4-PBT). This was due to the use of two mixers with different impeller types in one tank. In this variation, the 4-blade propeller is superior to the 4-pitched blade turbine because the distribution of pure axial flow is wider than the 4-pitched blade turbine, which produces a combined flow pattern [28]. At a speed of 300 rpm, a fairly large stagnant zone is visible on the upper left side, where the tracer is not circulated in that area due to the minimal flow range depending on the type of agitator, resulting in inefficient mixing [29]. However, as the impeller speed increases, the stagnant zone begins to narrow because the rapid flow distribution expands the fluid flow circulation. In the combination variation, the best flow pattern is concluded at a speed variation of 600 rpm, because the stronger turbulence from the 4-blade propeller can narrow the stagnant zone, although it is not better than using a dual-4 blade propeller.

The CFD simulation results show good agreement with the experimental findings. Each variable in both methods demonstrates an increase in fluid turbulence intensity as the impeller rotational speed increases from 300 rpm to 600 rpm. Among the three types of impellers tested, the best performance was obtained with the dual-PBT impeller at 600 rpm, both in visualization and simulation. This configuration produced a multiple-loop circulation flow pattern with a combined axial–radial flow and without any stagnant zones, resulting in a more effective mixing circulation that covered the entire tank and enhanced homogenization compared to other dual impeller designs.

The superior performance of the dual 4-PBT configuration can be explained by the hydrodynamic characteristics generated by its 45° pitched blades. Unlike the dual 4-blade propeller, which predominantly produces axial flow, the dual 4-PBT simultaneously generates both axial and radial flow components. The interaction between these flow components promotes stronger circulation patterns throughout the mixing tank, resulting in a more uniform distribution of momentum and solid particles. Furthermore, the radial discharge generated by the pitched blades enhances local shear and turbulence intensity, while the axial flow continuously transports the suspension between the upper and lower regions of the tank. Consequently, the enhanced axial–radial flow interaction improves overall flow circulation, reduces stagnant zones, promotes more effective solid suspension and mass transfer, and ultimately leads to shorter mixing times and better mixing homogeneity than the other impeller configurations investigated in this study. These findings are consistent with the study by [30] which demonstrated that a 45° pitched-blade impeller produced a more uniform flow field and turbulent kinetic energy distribution, thereby improving the hydrodynamic characteristics and mixing performance of the stirred tank.

A related study on computational and experimental investigation of a single top-entry mixing tank system using a 4-PBT impeller was conducted by Yanyan Cui *et al.,* (2018), the results indicated that the 4-PBT impeller generated a combination of axial–radial flow with high shear stress characteristics. However, a stagnant zone appeared near the impeller at 60 seconds, which gradually disappeared as the mixing time increased to 360 seconds. In contrast, the use of a side-entry tank with a dual-mixer configuration did not produce any stagnant zones from start to finish, owing to the twin circulation patterns and more uniform distribution, unlike the limited circulation observed in a single top-entry tank.

3.2.2 The Effect of Rotational Speed and Impeller Type on Fluid Distribution Contour

The distribution contour in the mixing process refers to the way the stirred materials spread throughout the flow domain in a stirred tank, visualized in the form of a concentration color gradient. The colors on this contour reflect the heterogeneity of the substances, such as in the solid-liquid mixing process. The red area reflects the high density of solids, while dark blue indicates the density of the solvent. As the stirring time increases, the red and blue areas slowly merge to form a light blue color, which indicates that concentration homogeneity has been achieved. Meanwhile, in the visual method, a gray scale is used, where black indicates $CaCO_3$ and clear indicates water. When homogeneous, the solution will turn dark gray, indicating that the two substances are uniform. Table 3 shows that of the three impeller types, the concentration color gradient began to appear uniform at 120 seconds for both the CFD and visual methods, except for the visual method, where the combination of the two impeller types showed that the concentration color gradient began to appear uniform at 140 seconds.

The insignificant differences in the contour distribution results for each method are due to the conditions and scale used in the simulation process being optimal, allowing the process to run stably. Meanwhile, in the experimental visualization in the laboratory, there are environmental factors such as light that can affect the clarity of the experimental results. In addition, surface wear on the impeller blades caused by the erosive impact of particles on the blade surface during the mixing of $CaCO_3$ and water resulted in a decrease in thickness, thereby reducing the circulation force [6]. Another factor may be the accuracy of the $CaCO_3$ particles used in laboratory experiments, where there are different particle shapes and the particle size distribution is not uniform [31]. According to a study by Li *et al.,* (2018), on side-entry flow simulation in large-scale biogas digesters, placing the mixer less than 8 cm from the tank bottom helps reduce sediment formation and promotes more uniform fluid distribution, thereby shortening mixing time. Since the study lacked experimental validation, the present research confirms these simulation findings through visual experimental comparison using a side-entry dual-mixer tank with an impeller height of 8 cm. The results can serve as a reference for future studies analyzing side-entry dual mixers with impeller heights below 8 cm.

3.2.3 Effect of Mixing Time on Fluid Density

Density measurements were taken to determine the homogeneity of the fluid and the mixing time. Density measurements were taken at three sampling points at heights of 5 cm, 20 cm, and 40 cm from the bottom of the tank every 60 seconds. Sampling at different heights aims to determine the distribution of fluid at each height, which will then provide homogeneity and mixing time values. The following are the density measurement results for each impeller type variation at rotation speeds of 300 and 600 rpm:

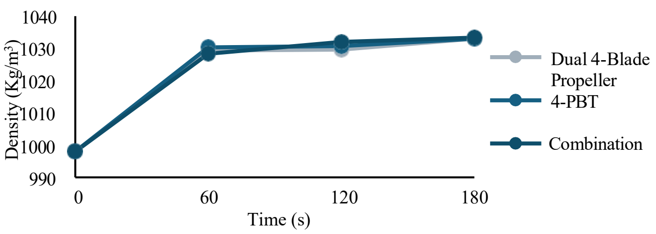

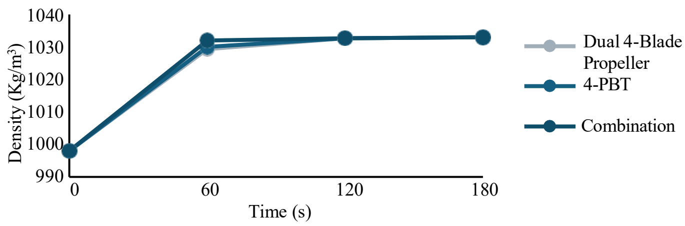

(a) (b)

Figure 5. Effect of Mixing Time on Fluid Density at Speeds of (a) 300 rpm and (b) 600 rpm

Based on Figure 5 above, it can be observed that the longer the stirring time, the density value tends to increase until it reaches a constant condition. In the variation of the dual 4-blade propeller and dual 4-PBT types at a speed of 300 rpm, the density results began to stabilize at 180 seconds, and at a speed of 600 rpm, the density began to stabilize at 140 seconds. Meanwhile, in the combination of both impeller types at a speed of 300 rpm, the density was not yet constant, but at a speed of 600 rpm, the density began to stabilize at 160 seconds.

The overall results show insignificant differences depending on the type of impeller used. Of the three variables, the combination variation was slower to reach a constant condition. This was because the use of two different types of impellers in one tank produced different flow circulations. The pure axial circulation of the 4-blade propeller proved to be stronger than the 4-PBT axial-radial combination, resulting in a large stagnant zone at the beginning of the stirring. When the density shows a constant number, it means that the solvent is saturated and there are no more significant changes in density even if stirring continues.

The best density measurement results were obtained with the dual 4-PBT variation at a 45° angle at a speed of 600 rpm, where the increase in density occurred more quickly because the wide axial-radial flow circulation could reach a constant value in a short time compared to other variables. In line with the research conducted by Wu *et al.*, (2023), related to measuring the quality of solid-liquid mixing using experimental image analysis methods, which showed that when the stirring speed was 260 rpm, the HMD value of the solid distribution when using a 2-pitched blade impeller was lower than when using a Rushton impeller, which means that a 2-pitched blade impeller contributes to a more even distribution. This is because the 2-pitched blade impeller produces a dispersed axial circulation compared to the Rushton impeller, which produces radial circulation. However, this research is limited to subjective experimental measurements, so validation using computational simulation is needed. Thus, this study proves that the use of impellers with a slope on each mixer produces a double axial circulation pattern that affects the wider flow distribution circulation and accelerates the uniformity of the use of a single top entry mixer system in the study. The density data obtained was processed to obtain a homogeneity value using the coefficient of variation approach.

The homogeneity value can be seen in Table 4, which shows that the higher the impeller rotation speed, the greater the fluid turbulence, so that $CaCO_3$ is distributed more quickly throughout the tank and the time required to achieve uniformity is shorter [32]. At the initial condition, the homogeneity value shows several 1, which consists of only pure solvent (water), without the distribution of dissolved particles ($CaCO_3$). This value reflects the perfect uniformity of one component, so that there is no variation in concentration in the system. As the stirring process continues, $CaCO_3$ begins to disperse in the solvent and causes the homogeneity value to fluctuate. However, after mixing for a certain period and all particles have been evenly distributed, the homogeneity value returns to 1. Several factors influence the homogeneity value in the mixing process, including speed, duration, blade geometry, temperature, the characteristics of the materials being mixed, as well as their composition and viscosity. Increases in mixing speed and temperature can accelerate the homogenization of a mixture, thereby making the mixing process more effective and efficient, and vice versa [33]. From Table 4 regarding homogeneity values, a comparison of the mixing times of the three types of impellers can be seen in Figure 6.

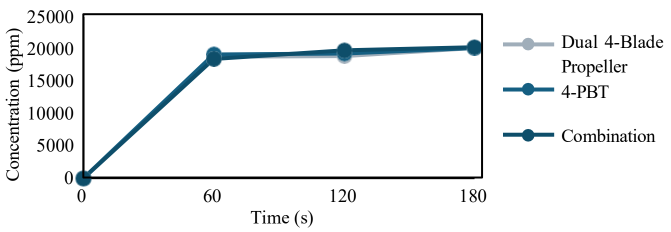

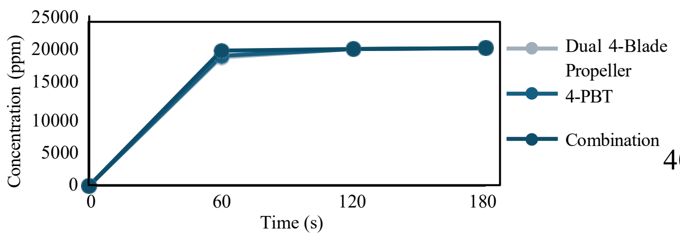

Figure 6. Comparison Chart of Mixing Time for the Three Types of Impellers

3.2.4 Effect of Mixing Time on $CaCO_3$ Concentration

Observations were made by measuring $CaCO_3$ concentrations using complexometric titration at various time intervals from the three sampling points. This was done to evaluate the extent to which $CaCO_3$ had dissolved and distributed evenly throughout the system, as well as to determine the mixing time required for the system to reach equilibrium. The following graph shows the relationship between $CaCO_3$ concentration and mixing time for each type of impeller:

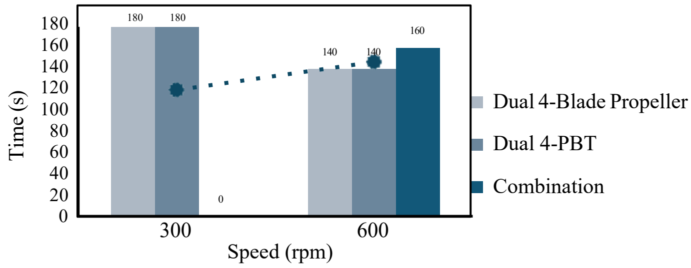

Figure 7. Effect of Stirring Time on $CaCO_3$ Concentration at Speeds of 300 rpm and 600 rpm

Based on Figure 7 above, it was found that the longer the stirring time, the longer the contact time between the sample and the solvent, resulting in a greater number of solids being mixed. This condition will continue until equilibrium is reached between the concentration of compounds in the raw material and the concentration of compounds in the solvent [34]. In addition, the higher the impeller rotation speed, the greater the effect on turbulence and convection within the system. As a result, the mass transfer process between the solid and liquid phases is faster, so that the time required to achieve uniformity in concentration distribution is shorter [35].

At a speed of 300 rpm, the equilibrium concentration is relatively slow, indicating that the mixing process is dominated by molecular diffusion. Meanwhile, at a speed of 600 rpm, the $CaCO_3$ concentration reaches equilibrium more quickly, indicating that the mixing process is dominated by convection due to increased shear forces and turbulence [36]. This condition causes the distribution of solid particles in the liquid to occur more quickly and efficiently, so that the system reaches homogeneity more quickly. The best configuration is obtained with dual 4-PBT at a speed of 600 rpm, which shows that the concentration has reached equilibrium in a shorter time, namely 120 seconds from a speed of 300 rpm.

3.2.5 Reynolds Number Correlation

The calculation of the Reynolds number aims to determine the level of fluid turbulence, so that the type of fluid flow can be predicted [22]. Table 5 shows the results of the Reynolds number for each type of impeller, which increases with the increase in the speed of the agitator. Each impeller type variation—dual 4-blade propeller, dual 4-PBT, and a combination of 4-blade propeller and 4-PBT—produced laminar flow at 300 rpm and transitional flow at 600 rpm. However, even though the type of flow obtained was the same from the three impeller types, they had different Reynolds numbers. The highest Reynolds number was obtained by the dual 4-PBT type at a rotational speed of 600 rpm, which was 3127.19, classified as transitional flow.

Laminar flow (Re < 2100) typically exhibits dominant shear stress and minimal turbulence, so mixing occurs only through molecular diffusion, which tends to be slow. In contrast, transitional flow (2100 < Re < 4000) has an unstable flow structure with increased convection that triggers more effective mass diffusion. In line with research conducted by Adnan *et al*., (2017), it was found that increasing the impeller speed can increase velocity fluctuations and local turbulence, as well as improve mixing efficiency by narrowing the dead zone to enter the transition range. This increase in turbulence also accelerates homogenization and significantly reduces mixing time.

4. Conclusions

Based on the results of the study, the type of impeller affects the flow circulation pattern, while increasing the impeller rotation speed accelerates the mixing time. The best flow pattern was obtained with a dual 4-pitched blade turbine impeller at 600 rpm. Both methods showed the formation of multiple axial-radial circulation loops without stagnant zones, resulting in effective mixing circulation with the fastest mixing time of 120 seconds. The visual experiment method was proven to provide flow pattern characteristics in line with the CFD results. The three impeller types: dual 4-blade propeller, 4-PBT, and a combination of both—produced different mixing times and homogeneity levels, influenced by speed variations. The higher the impeller speed, the faster the homogenization process of the CaCO3 and water mixture in the Side Entry Dual Mixer. Additionally, an increase in the Reynolds number was found to reduce the mixing time due to increased flow turbulence. The highest Reynolds value was also obtained in the dual 4-PBT at 600 rpm, which was 3127.19, falling into the transitional flow category. These findings are consistent with previous studies that mention that increasing the impeller speed increases velocity fluctuations, local turbulence, and mixing efficiency by minimizing the dead zone. Further research can explore the use of tracer particles and different types of impellers and fluids to optimize the design of side entry mixers.

Acknowledgment

This research was financially supported by the Final Project Assistance Grant (Bantuan Tugas Akhir Mahasiswa) funded by Institut Teknologi Sepuluh Nopember (ITS) under the 2025 ITS Internal Research Grant Scheme.

References

[1] S. Madhania, N. N. Fathonah, Kusdianto, T. Nurtono, and S. Winardi, “Turbulence Modeling in Side-Entry Stirred Tank Mixing Time Determination,” *MATEC Web Conf.*, vol. 333, p. 02003, 2021, doi: 10.1051/matecconf/202133302003.

[2] M. Cortada-Garcia, V. Dore, L. Mazzei, and P. Angeli, “Experimental and CFD studies of power consumption in the agitation of highly viscous shear thinning fluids,” *Chem. Eng. Res. Des.*, vol. 119, pp. 171–182, 2017, doi: 10.1016/j.cherd.2017.01.018.

[3] Rusiyanto *et al.*, “Pengaruh Durasi Pencampuran Terhadap Mechanical Properties Crucible,” *Tek. Mesin*, no. 1, pp. 39–64, 2022.

[4] H. P. Bayu, R. Gatut, and S. Untung, “Pengaruh Jumlah Sudu Pengaduk Terhadap Pola Pencampuran dan Konsumsi Daya Listrik pada Mixer Vertikal,” *J. V-Mac*, vol. 5, no. 1, pp. 9–12, 2020.

[5] N. N. Fathonah, T. Nurtono, Kusdianto, S. Madhania, Wahyudiono, and S. Winardi, “Numerical study of the hydrodynamic characteristics in an agitated tank with side-entry mixer: The effect of stirrer entry

angle," *Int. J. Technol.*, vol. 10, no. 3, pp. 521–530, 2019, doi: 10.14716/ijtech.v10i3.2925.

[6] T. Jirout and D. Jiroutová, "Application of theoretical and experimental findings for optimization of mixing processes and equipment," *Processes*, vol. 8, no. 8, 2020, doi: 10.3390/PR8080955.

[7] N. Valentino, D. L. Hakim, and F. M. Yanti, "PERANCANGAN GEOMETRI DAN POWER PENGADUK UNTUK BIOREAKTOR," *J. Energi dan Lingkung.*, vol. 16, no. 2, pp. 55–58, 2020.

[8] M. Jaszczur, A. Młynarczykowska, and L. Demurtas, "Effect of Impeller Design on Power Characteristics and Newtonian Fluids Mixing Efficiency in a Mechanically Agitated Vessel at Low Reynolds Numbers," *Energies*, vol. 13, no. 3, pp. 1–19, 2020, doi: doi:10.3390/en13030640.

[9] S. E. Perangin-angin, A. Hamsi, Mahadi, Tugiman, D. Sitompul, and Indra, "Komponen-Komponen Dan Peralatan Bantu Mixer Kapasitas 6,9 Liter Putaran 280 Rpm," *Dinamis*, vol. 3, no. 4, p. 14, 2015, doi: 10.32734/dinamis.v3i4.7003.

[10] P. J. Cullen, R. J. Romañach, N. Abatzoglou, and C. D. Rielly, "Pharmaceutical Blending and Mixing," *Pharm. Blending Mix.*, pp. 1–490, 2012, doi: 10.1002/9781118682692.

[11] A. H. Wahyujati and H. Fandinuari, "Visualisasi Makro Instabilitas Pola Alir Serta Pengukuran Pumping Capacity Dan Mixing Time Dalam Tangki Berpengaduk Dengan Side Entering Impeller," pp. 1–119, 2015.

[12] N. Mumtazah, A. R. Putraninghadi, and N. Nisbatul, "Computational Liquid Dynamic Simulation Mixing Time from Side Inlet Mixer Tank," *PROZIMA (Productivity, Optim. Manuf. Syst. Eng.*, vol. 5, no. 1, pp. 30–40, 2021, doi: 10.21070/prozima.v5i1.1505.

[13] X. Xiong, Z. Liu, C. Tao, Y. Wang, and F. Cheng, "Numerical Simulation of Dense Solid-Liquid Mixing in Stirred Vessel with Improved Dual Axial Impeller," *Separations*, vol. 9, no. 5, 2022, doi: 10.3390/separations9050122.

[14] D. Xia, Z. Mao, S. Zhou, X. He, and Y. Wang, "Optimized Design of Solid-Liquid Dual-Impeller Mixing Systems for Enhanced Efficiency," *ACS Omega*, vol. 8, no. 50, pp. 47635–47645, 2023, doi: 10.1021/acsomega.3c05762.

[15] H. T. Ahngari, P. Noeparvar, and J. S. Moghaddas, "The effect of impeller type on the mixing time of the non-Newtonian fluids in stirred tanks," *Chem. Technol.*, vol. 11, no. 4, pp. 123–132, 2016.

[16] S. Madhania *et al.*, "Mixing behaviour of miscible liquid-liquid multiphase flow in stirred tank with different marine propeller installment by computational fluid dynamics method," *Chem. Eng. Trans.*, vol. 56, pp. 1057–1062, 2017, doi: 10.3303/CET1756177.

[17] *et al.*, "Computational and experimental investigation of laminar flow mixing system in a pitched-blade turbine stirred tank," *Int. J. Agric. Biol. Eng.*, vol. 11, no. 4, pp. 94–101, 2018, doi: 10.25165/j.ijabe.20181104.2729.

[18] M. Azizah and I. M. Arsana, "Pengembangan Modul Computational Fluid Dynamic di Teknik Mesin Universitas Negeri Surabaya," *J. Pendidik. Tek. Mesin*, vol. 12, no. 02, pp. 37–42, 2021.

[19] H. J. Pant, "Applications of the radiotracers in the industry: A review," *Appl. Radiat. Isot.*, vol. 182, no. December 2020, p. 110076, 2022, doi: 10.1016/j.apradiso.2021.110076.

[20] H. Widodo, R. Saputra, and Puryadi, "ANALISA POWER OF HYDROGEN DAN KESADAHAN FEED WATER BOILER GUNA MENINGKATKAN EFISIENSI BOILER DI PT. DJARUM KUDUS," *Maj. Ilm. Gema Maritim, e-issn*, vol. 23, no. 2, pp. 164–168, 2021, [Online]. Available: www.e-journal.akpelni.ac.id,

[21] V. Uruba, "Reynolds number in laminar flows and in turbulence," *AIP Conf. Proc.*, vol. 2118, no. June, 2019, doi: 10.1063/1.5114728.

[22] Y. Darni, L. Liameri, M. Hanif, and N. Putra, "Pengaruh Bilangan Reynold pada Sintesis Bioplastik Berbasis Pati Sorgum dan Gelatin E," *Pros. Semin. Nas. Kulit, Karet dan Plast.*, vol. 7, pp. 55–68, 2018.

[23] G. A. Candrasa, A. N. Afandi, and A. Aripriharta, “Performance Evaluation Of Micro-Hydro Power Plant Based On A Case Study Of 2 × 650 Kw,” *1st Int. Conf. Technol. Informatics, Eng*, pp. 1–7, 2022.

[24] M. Akhondizadeh and M. Khajoei, “Study of the mixer performance under different mixing conditions,” *Jordan J. Mech. Ind. Eng.*, vol. 13, no. 4, pp. 243–246, 2019.

[25] W. L. Mccabe, J. C. Smith, and P. Harriott, *Unit Operations Of Chemichal Engineering*, vol. 11, no. 1. 1993.

[26] K. Priyadi, C. T. Lu, and H. Sutanto, “Optimization of impeller design for stirred tank using computational fluid dynamics,” *IOP Conf. Ser. Mater. Sci. Eng.*, vol. 567, no. 1, 2019, doi: 10.1088/1757-899X/567/1/012032.

[27] M. W. Junuansyah, Chairul, and Drastinawati, “PENGARUH JENIS PENGADUK DAN WAKTU FERMENTASI PADA PEMBUATAN BIOETANOL DARI SARI NENAS REJECT,” *JOM FTEKNIK*, vol. 2, pp. 306–312, 2024.

[28] A. D. Saputra, A. Pratoto, G. Gusriwandi, and J. Suprianto, “The Effect of Tilt Angle of Axial Fan Blades on Air Flow Distribution in the Cabinet Dryer: Simulation Study Using Computational Fluid Dynamics,” *Teknomekanik*, vol. 4, no. 1, pp. 8–13, 2021, doi: 10.24036/teknomekanik.v4i1.8772.

[29] A. K. Dutt and A. Datta, “Imperfect mixing and dead-zone effects in nonlinear dynamics: Law of mass action revisited,” *J. Phys. Chem. A*, vol. 102, no. 41, pp. 7981–7983, 1998, doi: 10.1021/jp982629i.

[30] Y. Wu, P. You, and P. Luo, “Effect of pitched short blades on the flow characteristics in a stirred tank with long-short blades impeller,” *Chinese J. Chem. Eng.*, vol. 45, pp. 143–152, 2022, doi: 10.1016/j.cjche.2021.11.010.

[31] W. Fornari, F. Picano, and L. Brandt, “The effect of polydispersity in a turbulent channel flow laden with finite-size particles,” *Eur. J. Mech. B/Fluids*, vol. 67, pp. 54–64, 2018, doi: 10.1016/j.euromechflu.2017.08.003.

[32] S. Islam and M. Danish, “Effect of Rotational Speed on Liquid-Solid Mixing and Operating Conditions Smart tower cranes View project Environmental study View project Effect of Rotational Speed on Liquid-Solid Mixing and Operating Conditions,” *J. Comput. Technol.*, vol. 6, no. January, pp. 9–12, 2017, [Online]. Available: https://www.researchgate.net/publication/313839541

[33] A. Arifin and A. B. Sulong, “Effect of mixing parameters on the mixing time and density of composite HA/Ti6Al4V feedstock for powder injection molding,” *MATEC Web Conf.*, vol. 101, 2017, doi: 10.1051/matecconf/201710103003.

[34] Rajian Sobri Rezki, Dwimas Anggoro, and Siswarni MZ, “EKSTRAKSI MULTI TAHAP KURKUMIN DARI KUNYIT (Curcuma domestica Valet) MENGGUNAKAN PELARUT ETANOL,” *J. Tek. Kim. USU*, vol. 4, no. 3, pp. 29–34, 2015, doi: 10.32734/jtk.v4i3.1478.

[35] X. Zhang *et al.*, “Machine Learning-Based Impact of Rotational Speed on Mixing, Mass Transfer, and Flow Parameter Prediction in Solid–Liquid Stirred Tanks,” *Processes*, vol. 13, no. 5, 2025, doi: 10.3390/pr13051423.

[36] F. Montagnaro, “Sherwood (Sh) Number in Chemical Engineering Applications—A Brief Review,” *Energies*, vol. 17, no. 17, 2024, doi: 10.3390/en17174342.